

MASTER

PHOTODETACHMENT CROSS SECTIONS FOR He^- (4P^0)R. N. Compton, G. D. Alton, and D. J. Pegg*
Oak Ridge National Laboratory,
Oak Ridge, Tennessee 37830Summary

We report the first measurements of photodetachment cross sections for He^- (formed through charge exchange of He^+ with Ca vapor) over the photon energy range from 1.77 to 2.75 eV. The energies of auto-detached electrons from the metastable He^- beam have also been determined for the first time. The auto-detached electron energy agrees within experimental error (± 0.25 eV) with the known $1s2s2p$ 4P^0 He^- energy level. This taken with measurements for the lifetime of He^- infers that charge exchange of He^+ with Ca vapor produces 4P^0 He^- .

Negative helium ions were first detected in a mass spectrometer in 1939 by Hiby.¹ This surprising observation required the He^- ions to be extremely long-lived ($\gtrsim 1 \mu\text{s}$). In 1955 Holøien and Midtdal² argued that the 4P^0 $5/2$ state of $(1s2s2p)$ 4P^0 He^- is stable against autodetachment and might explain Hiby's observation of long-lived He^- ions. They further calculated that 4P^0 He^- is bound relative to $(1s2s)$ 3^S by 0.075 eV. Table I provides a summary of more recent calculations and one experimental measurement of the energy level of 4P^0 He^- .

Table I. Energy Levels for 4P^0 He^-

$E(1s2s)$ 3^S - $E(1s2s2p)$ 4^P (eV)	$E(1s2s2p)$ 4^P (eV)	Reference
$\gtrsim 0.075$	19.744	2 (Theo.)
$\gtrsim 0.033$	19.786	3 (Theo.)
0.067	19.752	4 (Theo.)
0.080 ± 0.02	19.739	5 (Exp.)
0.0774 ± 0.0003	19.7417	6 (Theo.)

Riviere and Sweetman⁷ in 1960 were the first to show that the He^- ion had a finite lifetime. The $4\text{P}_{3/2,1/2}$ level can decay through spin-orbit and spin-spin interaction via coupling with the doublet P states while $4\text{P}_{5/2}$ He^- can decay only through the considerably weaker spin-spin interaction. Blau, Novick, and Weinflash⁸ established that the $J=5/2$ lifetime is $345 \pm 90 \mu\text{s}$ and that a weighted average of the $J=3/2$ and $1/2$ lifetimes is $11 \mu\text{s}$. Table II presents a summary of measured lifetimes for He^- ions produced in a variety of collisions.

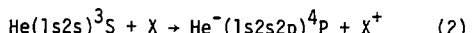
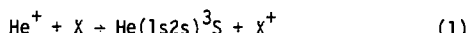
*Also Physics Department, University of Tennessee, Knoxville, Tennessee 37916

Table II. Measured Lifetimes of He^-

Source of He^-	Lifetime (μs)	Reference
$\text{He}^+ + \text{He}$	18.2	9
$\text{He}^+ + \text{N}_2$	9^{+5}_{-3}	10
$\text{He}^+ + \text{K}$	11.5 ± 5 , 345 ± 90	8
$\text{He}^+ + \text{K}$	10 ± 2 , 16 ± 4 , 500 ± 200	11
$\text{He}^+ + \text{Ca}$	10.5 ± 2	Present

The theoretical values for the lifetime of the $4\text{P}_{5/2}$ state of He^- are 303 , 12 505 , 12 266 , 13 and 455 ¹⁴ μs with the latter values of Estberg and LaBahn¹⁴ expected to be the most accurate. This value is in good agreement with the experimental values shown in Table II. Manson¹⁵ using wave functions which are less accurate than Estberg and LaBahn obtained 10^{-3} s for the $4\text{P}_{3/2}$ state but was unable to estimate the lifetime of $4\text{P}_{1/2}$ He^- . Manson further predicted that the energy for the fine structure levels would increase with J and that the energy excess Δ_{53} and Δ_{51} of the $5/2$ level above the $3/2$ and $1/2$ levels would be 8.43×10^{-6} eV and 3.89×10^{-5} eV. Mader and Novick¹⁶ used magnetic resonance techniques to determine Δ_{53} to be 3.41×10^{-6} eV and Δ_{51} to be 3.58×10^{-5} eV.

Donnally and Thoeming¹⁷ were the first to demonstrate that He^- could be produced in a two step process, i.e.,



where X is a target atom. The alkali atoms are the most efficient electron donors. Very large beam currents can be generated in this manner. Hooper et al.,¹⁸ for example, have been able to produce 70 mA pulses (10 ms pulse length) by charge exchange in sodium at 10.5 kV. Most tandem accelerator charge exchange sources can inject microampere beams of He^- .

Until about 1975, it was generally assumed that long-lived He^- ($\tau > 10^{-6}$ s) ions exist only in the $(1s2s2p)$ 4^P state. Three groups^{19,20,21,22} have recently raised the question of whether He^- may also exist in a long-lived doublet state. This conjecture was based on the fact that He^+ can pick up two electrons from an atom or molecule with closed s shells (i.e., $\text{He}^+ + \text{Ca} \rightarrow \text{He}^- + \text{Ca}^{++}$). More recent calculations⁶ dispute these conjectures since no long-lived 2^P states of He^- were obtained.

DISCLAIMER

This book was prepared as an account of work sponsored by an agency of the United States Government. Neither the United States Government nor any agency thereof, nor any of their employees, makes any warranty, express or implied, or assumes any legal liability or responsibility for the accuracy, completeness, or usefulness of any information, apparatus, product, or process disclosed, or represents that its use would not infringe privately owned rights. Reference herein to any specific commercial product, process, or service by trade name, trademark, manufacturer, or otherwise, does not necessarily constitute or imply its endorsement, recommendation, or favoring by the United States Government or any agency thereof. The views and opinions of authors expressed herein do not necessarily state or reflect those of the United States Government or any agency thereof.

Previously, Compton et al.²³ measured the lifetime of He^- formed through collisions of He^+ and Ca vapor and found it to agree with earlier reported values for $\text{He}^-(1s2s2p)^4\text{P}_3/2,1/2$. This was taken to be evidence that the He^- is formed in a quartet state. We provide further evidence for assignment by energy analyzing the electrons which autodetach from He^- along the direction of the ion beam. The energy of the autodetached electrons matches that of the known energy level of the $(1s2s2p)^4\text{P}^0$ state to within our experimental uncertainty (± 0.25 eV).

In this paper we also report the first measurements of the photodetachment cross section for $\text{He}^-(1s2s2p)^4\text{P}^0$ in the visible region of the electromagnetic spectrum. Brehm et al.⁵ have shown that the 2s and 2p electrons in $\text{He}^-(4\text{P}^0)$ are bound by 1.22 and 0.077 eV. Therefore, for the photon energies employed in this study, photodetachment into either continua, $\text{He}^-(3\text{S}) + \text{e}$ or $\text{He}^-(3\text{P}) + \text{e}$ is possible.

Cross sections for photodetachment of $\text{He}^-(1s2s2p)^4\text{P}^0$ were determined with the experimental apparatus shown in Fig. 1. Negative helium beams of 10^{-7} and 10^{-6} were momentum analyzed prior to entering the experimental apparatus (Fig. 1). An einzel lens was used to focus the ion beam through a collimation system into a Faraday cup. The bottom plate of the parallel plate arrangement was biased negatively (typically voltage: 200 V) in order to sweep photoelectrons into the channel electron multiplier (CEM). The hole in the top plate was 6.3 mm in diameter and was made large in order to accept all of the photodetached electrons. The laser and ion beams are orthogonal and the electron signal into the CEM detector was maximized by adjusting the laser position along the beam and/or adjusting the bottom plate voltage. Ambient pressures in the interaction region were $0.5-2 \times 10^{-6}$ torr.

A flash lamp-pumped tunable dye laser ($\Delta\lambda \approx 1.6$ Å) was used to continuously tune the photon energy through the visible region of the electromagnetic spectrum. The dye laser wavelength and spectral profile were continuously recorded with an optical multichannel analyzer and the relative laser power was monitored with a photodiode. The photodiode and photodetachment

signals were recorded in separate channels of a boxcar averager and their real time signals were recorded vs wavelength on an x-y recorder. During all the measurements, neutral density filters were inserted into the laser beam to ensure that saturation and multiphoton effects were not occurring. The absolute power of the laser was periodically measured in order to record the dye degradation which was found to be severe for the blue dyes. The laser energy per pulse was ~ 0.1 to 0.3 J at the peak of the dye curve and the laser typically operated at 10 pulses per second. Eight different dyes were used to scan the spectrum. All signals were recorded in real time - a typical dye scan took ~ 5 min. Relative cross sections were recorded for each dye by dividing the photoelectron signal by the photodiode signal and correcting for the known wavelength sensitivity dependence of the photodiode. The electron signal arriving at the electron multiplier was produced by collisionally detached, autodetached, and photodetached electrons.

During the $\sim 1 \mu\text{s}$ time for which the laser was on, the number of collisionally detached electrons was completely negligible at a background pressure of $\sim 1 \times 10^{-6}$ torr. The ratio R of the number of photodetached electrons to autodetached electrons during the time, t , that the laser is on is given by

$$R = N(h\nu)\sigma\tau / V(1 - e^{-t/\tau}) \quad (3)$$

where V is the interaction volume of the ion and laser beam, τ is the photon path length through the ion beam, $N(h\nu)$ is the number of photons in the laser pulse, σ is the photodetachment cross section, and τ is the lifetime ($\tau \approx 10 \mu\text{s}$) of $\text{He}^-(4\text{P}^0_{3/2,1/2})$. Using a laser intensity of 0.1 J/pulse (typical) and a cross section of $5 \times 10^{-18} \text{ cm}^2$, the ratio of signal to noise is ~ 100 . Therefore by using a high-powered pulsed dye laser and gating the boxcar integrator on only during the time the laser is on, background noise due to autodetachment is eliminated. Autodetachment backgrounds can, however, present serious difficulties in experiments using low-powered cw dye lasers.

Absolute photodetachment cross sections were determined by calibration of the data with known²⁴ cross sections for photodetachment of O^- which are accurate to $\pm 3\%$. Beams of O^- and He^- of known intensities were alternately introduced into the photodetachment region and the relative photodetachment signals $S_e(\text{O}^-)$ and $S_e(\text{He}^-)$ were recorded. The cross sections for photodetachment of He^- were then determined from

$$\sigma(\text{He}^-) = \frac{S_e(\text{He}^-)}{S_e(\text{O}^-)} \frac{I(\text{O}^-)}{I(\text{He}^-)} \frac{v_{\text{He}^-}}{v_{\text{O}^-}} \sigma(\text{O}^-) \quad (4)$$

where $I(\text{O}^-)$ and $I(\text{He}^-)$ are the beam intensities of O^- and He^- , respectively, and v_{He^-} and v_{O^-} are the velocities of the two ion beams. The photoelectron signal was also normalized to variations of laser intensity.

Measurements of autodetaching electron energies were accomplished by inserting a high resolution, spherical sector, electrostatic energy analyzer in place of the parallel plate arrangement shown in Fig. 1. The He^- beam was further collimated and allowed to pass through the analyzer, exiting through a gridded hole in the outer sphere of the analyzer and monitored in the Faraday cup. A simplified sketch of the experimental geometry is shown in Fig. 2. The energy of the

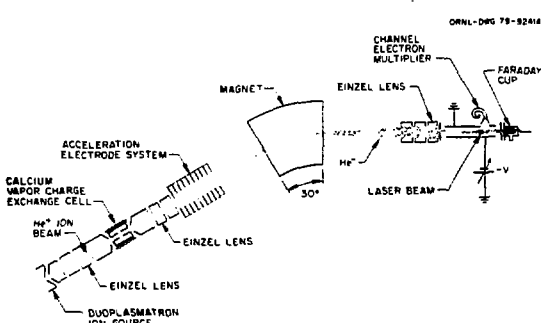


Figure 1. Experimental apparatus. Not shown are the flash lamp-pumped dye laser, optical multichannel analyzer, and photodiode. The autodetached electron energies were determined with a double focusing electrostatic energy analyzer inserted in place of the parallel plate detector (see Figure 2).

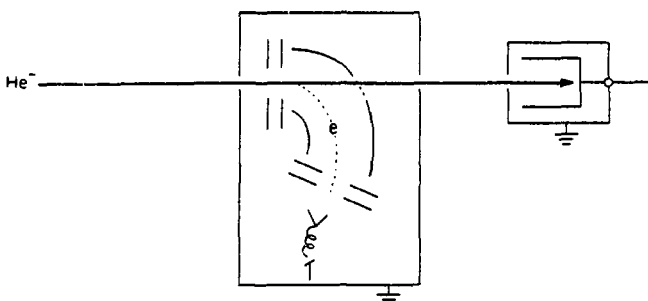


Figure 2. Experimental sketch of double focusing hemispherical electron energy analyzer arrangement used to measure autodetached and collisionally detached electrons from He^- ion beams.

autodetached electrons was calibrated relative to the collisionally detached or "cusp" electrons which were produced upon introducing a small amount of N_2 gas ($\sim 5 \times 10^{-6}$ torr) into the experimental chamber. The velocity of the electrons at the peak of the "cusp" was equated to the He^- ion velocity. The energy of the peak of the "cusp" electrons is equal to the ratio of the electron mass to helium mass times the ion energy. The energy of the He^- ion energy was measured with the aid of two independent precision electrostatic voltmeters and was believed accurate to within $\pm 5\%$. A plot of electron energy vs ion energy gives a straight line with a slope of 1.33×10^{-4} compared to $M_e/M_{\text{He}} = 1.3587 \times 10^{-4}$.

The electron energy intercept for zero ion kinetic energy is also zero indicating that contact potential in the energy analyzer are negligible on the scale of ~ 0.2 eV. A sample "cusp" electron energy spectrum for 40 KeV He^- ion energy is shown in Fig. 3. A rather large zero energy peak also accompanies the collisionally stripped electrons. These are presumably the result of collisions of He^- with apertures used to define the beam. The exact origin of these zero energy electrons will be the subject of further studies. Figure 4 shows the autodetached electron peaks for incident ion energies between 40 and 100 KeV. These runs were taken with a spectrometer resolution of ~ 0.5 eV, the best runs were taken with a resolution (FWHM) of ~ 0.2 eV. The energy scale shown in Fig. 4 is uncalibrated and was eventually calibrated with the "cusp" electron energy.

The autodetached energy, E_a , is related to the He^- ion kinetic energy E_i through the kinematic expression

$$E = E_c + 2 \sqrt{M_e/M_{\text{He}}} \sqrt{E_i E_a} + E_a \quad (5)$$

where E_i is the electron energy at the peak of the "cusp," i.e., $E_c = (M_e/M_{\text{He}})E_i$. Using this expression and data taken over the range of ion energies from 20 to 100 KeV, we find the autodetachment energy to be ~ 0.15 eV lower than the known energy level for He^{-4p_0} (see Table 1). This is within our experimental uncertainty of ± 0.25 eV. Any long-lived doublet state is expected to be well above the $4p_0$ state. Also, no other peaks are observed within an energy range of ± 5 eV about the observed peak. This provides direct evidence that long-lived He^- formed through charge exchanging collisions of He^+ and Ca vapor is primarily

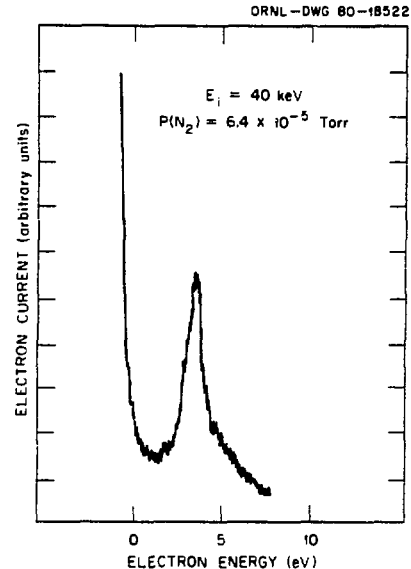


Figure 3. Plot of collisionally detached "cusp" electrons as a function of electron energy. The large rise in electron current at low energies is due to electrons stripped from the He^- due to collisions with apertures used to define the He^- ion beam.

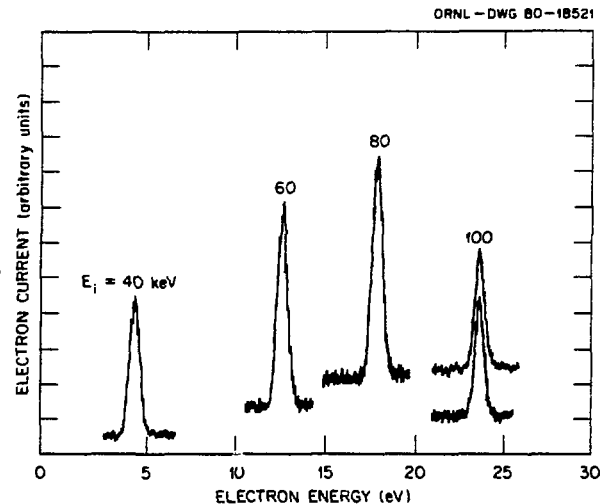


Figure 4. Plot of autodetached electron energy for various ion energies. The kinematic expression giving the electron energy as a function of ion energy and autodetachment energy is given in Eq. (5). The ion energy is only approximate, also the electron kinetic energy does not include the electron pass energy through the energy analyzer.

in the $(1s2s2p)^4p_0$ state. This, of course, implies that the Wigner spin conserving rule is violated in these collisions unless the He^+ picks up two electrons from different Ca targets. Data of others¹⁹⁻²² suggest that both electrons are transferred from a single target. We ourselves could not easily test this point.

The fact that the lifetime and energy level of the He^- formed in the collision $\text{He}^+ + \text{Ca} \rightarrow \text{He}^- + \text{Ca}^{++}$ matches the earlier lifetimes and known energy levels for ${}^4\text{P}^0 \text{He}^-$ strongly suggests but does not in itself rigorously prove that our He^- beam is in the ${}^4\text{P}^0 \text{He}^-$ state. Pedersen et al.²¹ earlier made the suggestion that "It is possible that the 10 μs component, which was ascribed to the $J=1/2$ and $3/2$ fine-structure components of the ${}^4\text{P}^0$ state, is in fact the ${}^2\text{P}^0$ state." The $(1\text{s}2\text{p})^2 {}^2\text{P}^0 \text{He}^-$ state would radiate to a lower lying $(1\text{s}2\text{s}2\text{p})^2 {}^2\text{P}^0$ state whose energy is close to that of ${}^4\text{P}^0 \text{He}^-$. If this state is within 0.25 eV of the ${}^4\text{P}^0 \text{He}^-$ we could not distinguish the two states. Final, conclusive identification of our He^- state will come from energy analysis of the photoelectron energy distribution at a photon energy where photodetachment into both ${}^3\text{S}$ and ${}^3\text{P}$ final states are possible.

The measured cross sections for photodetachment of ${}^4\text{P}^0 \text{He}^-$ are displayed in Fig. 5. The value at 2.41 eV, represented by an open triangle, is an earlier estimate of the cross section from photoelectron energy analysis studies⁵ and is in good agreement with the data presented in this study. The cross section is seen to increase by an order of magnitude from ~ 2.4 to 1.8 eV. Each data point is an average of from 2 to 7 measurements and we estimate the error associated with each data point to be $\pm 20\%$.

Photodetachment from photon energies above ~ 1.22 eV will result in both $\text{He}({}^3\text{S})$ and $\text{He}({}^3\text{P})$ final states. At 2.41 eV, Brehm et al.⁵ have shown that the ${}^3\text{S}$ state

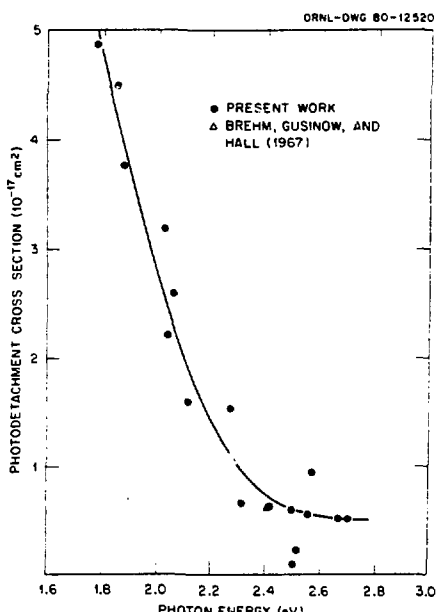


Figure 5. Photodetachment cross section for $\text{He}^-(1\text{s}2\text{s}2\text{p})$ ${}^4\text{P}^0$ vs photon energy.

is favored over the ${}^3\text{P}$ state by a factor of 7. This ratio is approximate since it is not corrected for anisotropies in the angular distribution of the two groups of photodetached electrons. Using known sum rules for photodetachment together with the cross sections shown in Fig. 2, we estimate that the total photodetachment cross section will exceed 10^{-16} cm^2 at longer wavelengths. Hodges et al.²⁵ have recently measured a photodetachment cross section of 1.2×10^{-16} at 0.12 eV using a CO_2 laser. Furthermore, using the principle of detailed balance, we predict rather large ($\geq 10^{-22} \text{ cm}^2$) radiative attachment cross sections for low-energy electrons to $\text{He}({}^3\text{S})$ atoms which are present in, say, a gaseous discharge environment like that where He^- was first observed.¹

We have searched for structures in the photodetachment cross section which might correspond to resonant excitation of higher compound quartet states of He^- . Continuous dye laser scans in the region from ~ 1.8 to 2.4 eV revealed no significant structures. Scatter in the data shown in Fig. 2 represents only statistical variations of cross section measurements. Calculations also provide no evidence for excited He^- states in this energy region. Transitions to the $\text{He}^-(1\text{s}2\text{p})^2 {}^4\text{P}^0$ would be allowed from the $\text{He}^-({}^4\text{P}^0)$ state; however, the expected transition energy $h\nu \approx 1.35 \text{ eV}$ ²⁶ is below that of our present laser capabilities.

A statistically significant variation in the cross section is seen at ~ 2.55 eV. Oberoi and Nesbet²⁷ have found theoretical evidence for a ${}^4\text{P}^0$ Feshbach resonance 0.18 eV below the ${}^3\text{S}$ threshold at 22.71 eV with a width of 0.05 eV. No ${}^4\text{S}$ resonance was found. However a $(1\text{s}3\text{s}3\text{d})^4\text{D}^0$ resonance was calculated to occur at 22.56 eV with a width of 0.01 eV. The He^- transition corresponding to ${}^4\text{P}^0 \rightarrow {}^4\text{D}^0$ is allowed and the feature at ~ 2.55 eV can be compared to the theoretical prediction²⁷ of 2.82 eV for this transition energy. However, we should point out that ${}^4\text{P}^0 \rightarrow {}^4\text{D}^0$ is a two electron excitation transition. The large uncertainties in both experiment and theory make any definite assignment tenuous at this point. More detailed studies of this wavelength region are in progress. We hope that this study will stimulate further theoretical work on magnitudes of photodetachment cross sections for $\text{He}^-({}^4\text{P}^0)$ and transition energies from $\text{He}^-({}^4\text{P}^0)$ to $\text{He}^-({}^4\text{L}^0)$ states.

Acknowledgments

The authors are greatly indebted to A. E. Carter for her dedicated technical assistance throughout all phases of the experiment.

Research sponsored by the Office of Health and Environmental Research, U.S. Department of Energy under contract W-7405-eng-26 with the Union Carbide Corporation.

References

1. Von Julius W. Hiby, Ann. Phys. 34, 473 (1939).
2. E. Holøien and J. Midtdal, Proc. Phys. Soc. London 68, 815 (1955).
3. E. Holøien and S. Geltman, Phys. Rev. 153, 81 (1967).
4. A. W. Weiss, Phys. Rev. 166, 70 (1968).
5. B. Brehm, M. A. Gusinow, and J. L. Hall, Phys. Rev. Lett. 19, 737 (1967).
6. A. V. Bunge and C. F. Bunge, Phys. Rev. 19, 452 (1979).
7. H. G. Riviere and D. R. Sweetman, Phys. Rev. Lett. 5, 560 (1960).
8. L. M. Blau, R. Novick, and D. Weinflash, Phys. Rev. Lett. 24, 1268 (1970).
9. D. J. Nichols, C. W. Trowbridge, and W. D. Allen, Phys. Rev. 167, 38 (1968).
10. F. R. Simpson, R. Browning, and H. B. Gilbody, J. Phys. B 4, 106 (1971).
11. R. Novick and D. Weinflash, Proc. Int. Conf. Precision Measurements and Fundamental Constants (Gaithersburg, Maryland), ed. D. N. Langenberg and B. N. Baylor, NBS Spec. Pub. 343, p. 403.
12. C. Laughlin and A. L. Stewart, J. Phys. B 1, 151 (1968).
13. G. N. Estberg and R. W. LaBahn, Phys. Lett. A 28, 420 (1968).
14. G. N. Estberg and R. W. LaBahn, Phys. Rev. Lett. 24, 1265 (1970).
15. S. T. Manson, Phys. Rev. A 3, 147 (1971).
16. D. L. Mader and R. Novick, Phys. Rev. Lett. 29, 199 (1972).
17. B. L. Donnelly and G. Thoeming, Phys. Rev. 159, 87 (1967).
18. E. B. Hooper, Jr., P. A. Pincosy, P. Poulsen, and C. F. Burrell, Rev. Sci. Instrum. 51, 1066 (1980).
19. R. A. Baragiola, abstracts of papers, VIII Int. Conf. Physics of Electronic and Atomic Collisions (Belgrade), p. 827 (1973).
20. R. A. Baragiola and E. R. Salvatelli, J. Phys. B 8, 382 (1975).
21. E. H. Pedersen, F. R. Simpson, and P. Hvelplund, J. Phys. B 7, L294 (1974); Phys. Rev. A 11, 516 (1975).
22. K. F. Dunn, B. J. Gilmore, F. R. Simpson, and H. B. Gilbody, J. Phys. B 11, 1797 (1978).
23. R. N. Compton, G. D. Alton, A. D. Williamson, and A. E. Carter, (abstracts of papers) XI Int. Conf. Physics of Electronic and Atomic Collisions (Kyoto, Japan), p. 68 (1979).
24. L. M. Branscomb, S. J. Smith, and G. Tisone, J. Chem. Phys. 43, 2906 (1965).
25. R. V. Hodges, H. J. Coggiola, and J. R. Peterson, private communication.
26. A. V. Bunge and C. F. Bunge, private communication.
27. R. S. Oberoi and R. K. Nesbet, Phys. Rev. A 8, 2959 (1973).